Structure−Function Relationships for Inhibitors of β-Amyloid Toxicity Containing the Recognition Sequence KLVFF[†]

Tao L. Lowe,[‡] Andrea Strzelec,[‡] Laura L. Kiessling,[§] and Regina M. Murphy*,[‡]

Departments of Chemical Engineering and Chemistry, University of Wisconsin, Madison, Wisconsin 53706

Received November 30, 2000; Revised Manuscript Received April 18, 2001

ABSTRACT: β-Amyloid (Aβ), the primary protein component of Alzheimer's plaques, is neurotoxic when aggregated into fibrils. We have devised a modular strategy for generating compounds that inhibit Aβ toxicity. These compounds contain a recognition element, designed to bind to Aβ, linked to a disrupting element, designed to interfere with Aβ aggregation. On the basis of this strategy, a hybrid peptide was synthesized with the sequence KLVFF (residues 16−20 of Aβ) as the recognition element and a lysine hexamer as the disrupting element; this compound protects cells in vitro from Aβ toxicity [Pallitto, M. M., et al. (1999) *Biochemistry 38*, 3570]. To determine if the length of the disrupting element could be reduced, peptides were synthesized that contained the KLVFF recognition element and a sequence of one to six lysines as disrupting elements. All compounds enhanced the rate of aggregation of Aβ, with the magnitude of the effect increasing as the number of lysines in the disrupting element increased. The greatest level of protection against Aβ toxicity was achieved with compounds containing disrupting elements of three or more lysines in sequence. A peptide with an anionic disrupting element, KLVFFEEEE, had activity similar to that of KLVFFKKKK, in both cellular toxicity and biophysical assays, whereas a peptide with a neutral polar disrupting element, KLVFFSSSS, was ineffective. Protective compounds retained activity even at an inhibitor:Aβ molar ratio of 1:100, making these some of the most effective inhibitors of Aβ toxicity reported to date. These results provide critical insight needed to design more potent inhibitors of Aβ toxicity and to elucidate their mechanism of action.

The primary proteinaceous component of senile plaques in Alzheimer's patients is β-amyloid peptide (Aβ),[1] a 39−43-amino acid fragment cleaved from the membrane-bound amyloid precursor protein (APP). Aβ is an amphiphilic peptide that spontaneously self-assembles into amyloid fibrils, a general term describing insoluble linear protein-aceous aggregates with diameters of ∼10 nm, cross-β-sheet conformation, and birefrigence upon staining with Congo red (*1*). These Aβ amyloid fibrils form the core of senile plaques. There is evidence that Aβ deposition predates other pathological events in Alzheimer's disease (*2*, *3*). Thus, deposition of Aβ is hypothesized to be a causative event in the development of Alzheimer's disease. This hypothesis is supported by genetic linkage studies (*4*) and transgenic mouse models (*5*, *6*).

Aβ is toxic to cells in culture. Specifically, several studies have demonstrated that conversion of monomeric Aβ to fibrils is required for Aβ toxicity (*7−9*). These and other results have led to the hypothesis that Aβ is toxic only when it is aggregated into insoluble fibrils. An alternative hypothesis that has gained significant exposure in recent years is one in which a soluble intermediate in the fibrillogenesis pathway is the toxic moiety, not the final insoluble product (*10−12*). Indeed, dimeric (*13*), oligomeric (*14*), and "protofibrillar" (*15*, *16*) Aβ are reportedly toxic to cultured cells. Although no general agreement has been reached on the exact identity of the toxic Aβ species, overwhelming evidence supports the hypothesis that, to be toxic, Aβ must be in an organized self-assembled state.

These observations suggest that prevention of Aβ aggregation may inhibit neuronal degeneration. Indeed, Congo red and related compounds (*17−19*), which have affinity for the cross-β-sheet structural domains typical of amyloid fibrils, possess inhibitory activity in Aβ aggregation and Aβ toxicity assays. Other compounds with reported antitoxicity and/or antiaggregation activity include conjugated cyclic compounds such as anthracyclines (*20*), rifampicin (*21*), benzofurans (*22*), and pyridones (*23*).

An alternative approach is to exploit the self-recognizing features of Aβ to generate compounds that can interact specifically with Aβ. Variations on this theme have been published by us (*10*, *24*) and others (*25−27*). In our approach, a fragment of Aβ is used which serves as a specific binding domain ("recognition element"). This recognition element is coupled to a separate domain, the "disrupting element", which serves to interfere with normal fibril self-

---

assembly. This modular design allows independent optimization of the two functional domains, and generates "hybrid" compounds that protect cells in vitro from Aβ toxicity. In the first successful implementation of this strategy, the sequence of residues 15−25 of Aβ was linked to a lysine hexamer (*24*). More recently, we reported that the sequence KLVFF (residues 16−20 in Aβ) served as an even more effective recognition element when coupled to the lysine hexamer-disrupting element (*10*). This hybrid peptide (KLVFFKKKKKK) fully protected PC-12 cells from Aβ toxicity at an Aβ:inhibitor molar ratio of 1:1. Strikingly, the hybrid inhibitor did not prevent Aβ aggregation; in fact, Aβ aggregation rates were dramatically enhanced. These results are significant because they suggest that compounds need not block aggregation to block Aβ toxicity. Moreover, the data suggest that the hybrid inhibitors may function by a mechanism which does not require 1:1 complexation with Aβ.

The objective of the work reported here is to further define the requirements for effective disrupting domains. Specific questions that are addressed include the following. (a) What is the minimum length requirement for the oligolysine-disrupting domain? (b) Can anionic or nonionic disrupting domains substitute for cationic domains? (c) How does protection against toxicity correlate with changes in Aβ aggregation? (d) Do hybrid compounds provide protection against Aβ toxicity at less than stoichiometric ratios? The answers to these questions will provide critical insight needed to design more potent inhibitors of Aβ toxicity and to elucidate their mechanism of action.

MATERIALS AND METHODS

Peptide Synthesis. Aβ(1−40) was purchased from AnaSpec, Inc. (San Jose, CA). Its purity and identity were assessed by amino acid analysis, mass spectrometry, and reverse phase HPLC; the reported purity was >95%, and the reported molecular mass was 4331.3 Da (theoretical molecular mass of 4330.9 Da). All other peptides were synthesized by solid phase peptide synthesis using Fmoc-protected amino acids and either HBTU- or HOBT-mediated coupling reactions. *N,N*-Dimethylformamide was purchased from Sigma-Aldrich (St. Louis, MO), and acetonitrile (HPLC grade) was purchased from Fisher Scientific (Fairlawn, NJ). HOBT, HBTU, protected amino acids, and resin were purchased from Novabiochem (La Jolla, CA) or Advanced ChemTech (Louisville, KY). Deprotected peptides were cleaved from the resin, and then purified by reverse phase HPLC on a C18 Vydac column using linear gradients of acetonitrile and water with 0.1% TFA as the mobile phase. Purified peptides were analyzed by MALDI mass spectrometry. Peptides were stored as lyophilized powders at −70 °C. Hybrid peptide sequences are listed in Table 1.

Cellular Toxicity. PC-12 cells (ATCC, Rockville, MD) were grown on polylysine-coated T-flasks in medium containing 85% RPMI 1640, 5% fetal bovine serum, 10% heat-inactivated horse serum, 3.6 mM L-glutamine, and a penicillin/streptomycin mixture, in a humidified incubator at 37 °C and 5% CO2. Medium components were from GibcoBRL (Grand Island, NY). Cells were harvested from T-flasks after brief treatment with trypsin (0.05% trypsin with 0.4 mM EDTA), resuspended in medium, and plated onto

Table 1: Hybrid Peptide Sequences

sequence	name	theoretical molar mass	measured molar mass
KLVFFK	KLVFF-K$_1$	781.0	781.5
KLVFFKK	KLVFF-K$_2$	909.2	909.5
KLVFFKKK	KLVFF-K$_3$	1037.4	1037.7
KLVFFKKKK	KLVFF-K$_4$	1165.6	1165.8
KLVFFKKKKKK	KLVFF-K$_6$	1421.9	1422.0
KLVFFEEEE	KLVFF-E$_4$	1169.3	1169.6
KLVFFSSSS	KLVFF-S$_4$	1001.2	1000.5

polylysine-coated 96-well plates at a density of 15 000 cells/well (100 μL/well). Plates were incubated at 37 °C for 24 h to allow cells to attach. Lyophilized Aβ was dissolved in 0.1% TFA at a concentration of 5−10 mg/mL at 37 °C for 1 h and then diluted into sterile-filtered phosphate-buffered saline (PBS) (0.01 M KH2PO4/K2HPO4 and 0.14 M NaCl) containing penicillin and streptomycin. Hybrid peptides were dissolved directly into sterile-filtered PBS with antibiotics (10 μL) and added to Aβ solutions. The final Aβ concentration was 0.5 mg/mL (115 μM); the peptide:Aβ molar ratio was 1:1 unless otherwise indicated, and the pH was 7.4. Samples were incubated without shaking at 37 °C for 48 h, and then diluted into fresh medium without phenol red (Sigma) supplemented with serum, L-glutamine, and antibiotics. Eighty percent (80 μL) of the medium was carefully removed from each well and replaced with 80 μL of medium (control) or 80 μL of medium containing Aβ or a peptide/Aβ mixture. The Aβ concentration in wells was 25 μM. Plates were incubated at 37 °C for 24 h. Cell viability was determined using the MTT assay. Briefly, 10 μL of MTT (5 mg/mL in RPMI medium without phenol red) was added to each well. After incubation for 4 h at 37 °C, 100 μL of a 50% dimethylformamide/20% sodium dodecyl sulfate (pH 4.7) mixture was added. The plates were incubated overnight at 37 °C, and then the absorbance at 570 nm was measured using a microplate reader (Bio-tek Instruments, Winooski, VT) with background subtraction. Cell viability was calculated by dividing the absorbance of wells containing Aβ or Aβ and peptide (corrected for background) by the absorbance of wells containing medium alone (corrected for background). Averages from seven replicate wells were used for each sample and control, and each experiment was repeated two to five times.

Laser Light Scattering. PBSA [PBS with 0.02% (w/v) NaN3 (pH 7.4)] was filtered through 0.22 μm filters. Aβ was dissolved in 0.1% TFA to a concentration of 10 mg/mL for 1 h, and then diluted into filtered PBSA. The hybrid peptide was dissolved in 10 μL of PBSA and the mixture added immediately to freshly diluted Aβ. The Aβ concentration was 0.5 mg/mL, and the peptide:Aβ molar ratio was 1:1 unless otherwise indicated. The pH was adjusted to 7.4 with NaOH, and then the solution was immediately filtered through 0.45 μm filters (Millipore, Bedford, MA) directly into a cleaned light scattering cuvette placed in a bath of the index-matching solvent decahydronaphthalene, which was temperature-controlled to 25 °C. Dynamic light scattering data were collected using a Lexel argon ion laser and a Malvern 4700 system, as described previously (*28*). Autocorrelation data at a scattering angle of 90° were collected over a period of hours to days. Data were fit to a third-order cumulants expression to derive an average apparent hydrodynamic diameter.

Static light scattering measurements were taken using the same samples and apparatus, as described in detail previously (*28*). Briefly, the scattered light intensity at 24 angles from 20° to 135° was collected twice for 10 s each time; each measurement was repeated 10 times and averaged. The average scattered intensity of the buffer was measured in the same manner and subtracted from the sample scattering intensity; the result was then normalized using the scattering intensity of a reference solvent (toluene) to obtain the Rayleigh ratio $R_s(q)$ as a function of scattering vector q, where $q = (4\pi n/\lambda_o) \sin(\theta/2)$, where n is the refractive index of the solvent, λ_o is the wavelength of the incident beam in vacuo, and θ is the scattering angle. Data were analyzed as described previously (*29*). Briefly, the data were plotted in the Kratky format, $q^2R_s(q)/Kc$ ($=q^2M_wP(q)$) versus q, where c is the peptide concentration, $K = 4\pi^2n^2(dn/dc)^2/N_A\lambda_o^4$, dn/dc is the refractive index increment (0.181 cm^3/g, assumed to be independent of aggregation state), N_A is Avogadro's number, M_w is the weight-averaged molecular weight, and $P(q)$ is the particle scattering factor, which is a function of particle shape. Two alternative models of particle shape, semiflexible (wormlike) chain and semiflexible (wormlike) branched, were used to fit the data. The semiflexible chain model describes a linear chain with a total contour length L_c and a Kuhn statistical segment length l_k (a measure of the stiffness of the chain, equal to 2 times the persistence length). $P(q)$ for semiflexible chains is

$$P(q) = \frac{2}{L_c^2}\int_2^{L_c}(L_c - t)\phi(t,l_k,q)\,dt \qquad (1)$$

where the function $\phi(t,l_k,q)$ has been described elsewhere (*29, 30*). We have shown previously that this model is a good description of Aβ fibrils (*28, 29*). The continuous semi-flexible branched model describes a branched particle with a center from which emanate f semiflexible chains of equal length ($f = 2$ for a linear chain). $P(q)$ is a function of l_k, the contour length of one arm $L_{c,a}$, and the number of branches f (*31*):

$$P(q) = \frac{1}{fL_{c,a}^2}[2(2 - f)\int_0^{L_{c,a}}(L_{c,a} - x)\phi\,dx +$$
$$(f - 1)\int_0^{2L_{c,a}}(2L_{c,a} - x)\phi\,dx] \quad (2)$$

M_w, l_k, L_c (or $L_{c,a}$), and, where appropriate, f were determined by nonlinear regression of the data as described previously (*10*).

Size Exclusion Chromatography. Aβ samples were prepared as described for the light scattering studies. The Aβ concentration was 0.5 mg/mL, and the Aβ:peptide molar ratio was 1:1. A 25 μL loop was filled with the sample and then the sample injected onto a Superdex 75 PC 3.2/30 column connected to a Pharmacia FPLC system (Amersham Pharmacia Biotech, Piscataway, NJ). PBSA at a rate of 0.05 mL/min served as the mobile phase, and Aβ-containing fractions were detected by absorbance at 280 nm. The hybrid peptides are not detected by absorbance at 280 nm. Injections were carried out in triplicate. The column was calibrated using the following proteins as molecular mass standards: insulin chain B (3.5 kDa), ubiquitin (8.5 kDa), ribonuclease A (13.7 kDa), ovalbumin (43 kDa), and bovine serum albumin (67
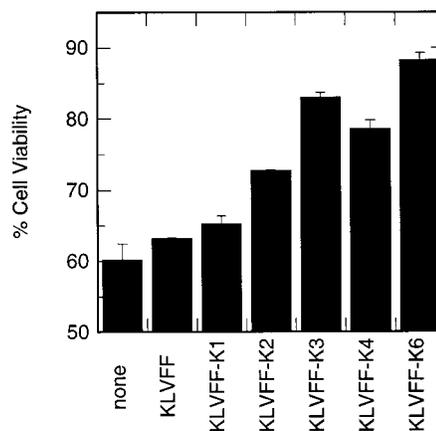
FIGURE 1: Effect of hybrid peptides with lysine-disrupting domains on cellular toxicity of Aβ solutions. Aβ alone ("none") or with the designated peptide was incubated for 2 days at 37 °C, and then added to plated PC-12 cells for 1 day. The Aβ concentration in wells was 25 μM, and the Aβ:hybrid molar ratio was 1:1. Cellular viability was assessed with the MTT assay. Each bar represents the mean ± standard deviation of results from two to eight runs, with seven replicates per run.

kDa). The fraction of Aβ eluting at a given retention time was calculated by dividing the integrated peak area at that retention time by the peak area of an Aβ sample injected without the column in place.

RESULTS

Activity of Compounds with the Variable-Length Oligo-lysine-Disrupting Element. Previously we observed that KLVFFKKKKKK (KLVFF-K$_6$) was effective at inhibiting Aβ toxicity in vitro (*10*). To determine whether shorter lysine-disrupting domains were equally effective, we examined the ability of oligolysine-containing hybrid peptides to inhibit toxicity of Aβ toward PC-12 cells, using an MTT assay. In agreement with previous results, Aβ alone (25 μM, aggregated for 2 days) caused a decrease in the level of MTT reduction to ~60% of control. When Aβ was mixed at a 1:1 molar ratio with hybrid peptides containing a contiguous sequence of one to six lysines, the viability of the treated cells increased with an increasing number of lysines in the inhibitor sequence (Figure 1). The recognition element alone (KLVFF) or a hybrid peptide containing a single lysine-disrupting element (KLVFFK$_1$) provided little to no protection. Significant protection was provided by those compounds containing at least three lysines in the disrupting element.

We next examined the relationship between the size of the oligolysine-disrupting element and the rate of Aβ aggregation. The average apparent hydrodynamic size and growth rate of aggregates formed in mixtures of Aβ with hybrid peptides were measured by dynamic light scattering, and compared to those of Aβ alone. All hybrid peptides containing an oligolysine-disrupting domain caused an increase in aggregate growth rate compared to that of Aβ alone (Figure 2), with the rate of increase strongly dependent on the length of the oligolysine element. The time required for formation of visible precipitates decreased dramatically as the length of the lysine string increased (Figure 2 inset).

To further characterize the size and shape of aggregates, we collected and analyzed static light scattering (SLS) data for solutions of Aβ alone or with hybrid peptides. Data taken 1 h after mixing are shown as Kratky plots in Figure 3. The
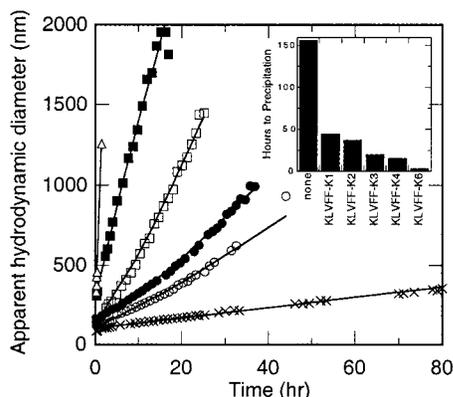
FIGURE 2: Effect of hybrid peptides with lysine-disrupting elements on the aggregation kinetics of Aβ solutions. Aβ was mixed with the indicated peptide at 115 μM Aβ and a 1:1 Aβ:peptide molar ratio. The average apparent hydrodynamic diameter was determined by cumulants analysis of autocorrelation functions collected at a scattering angle of 90°: (×) Aβ alone, (○) Aβ with KLVFF-K$_1$, (●) Aβ with KLVFF-K$_2$, (□) Aβ with KLVFF-K$_3$, (■) Aβ with KLVFF-K$_4$, and (△) Aβ with KLVFF-K$_6$. The inset shows the approximate time before observation of visible macroaggregates.
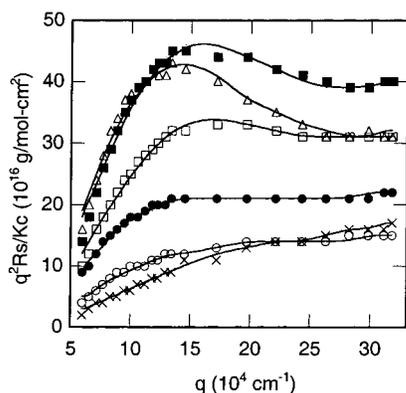
FIGURE 3: Effect of hybrid peptides with lysine-disrupting elements on the scattering intensity of Aβ-peptide solutions. Data were collected 1 h after mixing and are presented in the form of Kratky plots (see the text). In each case, Aβ was mixed with the designated peptide at 115 μM Aβ and a 1:1 Aβ:peptide molar ratio: (×) Aβ alone, (○) Aβ with KLVFF-K$_1$, (●) Aβ with KLVFF-K$_2$, (□) Aβ with KLVFF-K$_3$, (■) Aβ with KLVFF-K$_4$, and (△) Aβ with KLVFF-K$_6$. The lines are fits of eq 1 or 2 to experimental data.

Kratky plot is a convenient means for distinguishing between linear versus branched structures for particles with characteristic dimensions on the order of the wavelength of the incident beam (*32*). In this plot, an increase in the *y*-axis intercept is indicative of an increase in molecular mass. The shape of the curve is indicative of the particle shape; specifically, a curve with a plateau is typical of a linear semiflexible chain, whereas a curve with an intermediate "bump" is typical of a branched structure. Previous work indicated that morphological information extracted from analysis of Kratky plots was consistent with electron microscope images (*24*). As shown in Figure 3, there is a clear increase in the average molecular weight, and an indication of a shift from a linear to a branched morphology, when Aβ is mixed with hybrid peptides with oligolysine sequences of increasing length.

The data were fit by nonlinear regression to eqs 1 and 2. The fitted curves are plotted along with the data in Figure 3, and the parameter values are summarized in Table 2. Data for Aβ alone, or Aβ mixed with KLVFF-K$_1$ or KLVFF-K$_2$,

Table 2: Size Characteristics of Aβ Aggregates in the Presence of Hybrid Peptides 1 h after Mixing[a]

added peptide	$\langle M \rangle_w$ ($\times 10^6$ g/mol)	L_c (nm)	l_k (nm)	f	$\langle M \rangle_w/L_c$[b] ($\times 10^3$ g mol^{-1} nm^{-1})
none	8.7 ± 0.5	400 ± 20	270 ± 50	ND	22 ± 2
KLVFF-K$_1$	17 ± 1	960 ± 40	140 ± 10	ND	17 ± 2
KLVFF-K$_2$	40 ± 2	1800 ± 400	110 ± 20	ND	22 ± 4
KLVFF-K$_3$	40 ± 2	1300 ± 400	130 ± 40	4 ± 1	30 ± 9
KLVFF-K$_4$	60 ± 4	1400 ± 400	140 ± 40	4 ± 1	40 ± 10
KLVFF-K$_6$	69 ± 4	2000 ± 500	130 ± 430	5 ± 1	35 ± 10

[a] Parameter values were determined by fitting data in Figure 3 to eq 1 or 2. Error estimates are 95% confidence intervals for the data fits. [b] The ratio $\langle M \rangle_w/L_c$ is calculated by dividing $\langle M \rangle_w$ by L_c, with the error calculated by propagation-of-error analysis. $\langle M \rangle_w$ includes contributions from monomers, dimers, and oligomers as well as fibrils; therefore, the ratio does not reflect a true measure of the linear density.

were well fit by the linear model ($f = 2$), consistent with a nonbranching fibrillar structure. ("fibrillar" is used to describe any long chainlike Aβ aggregate; no distinction is made between filaments, protofibrils, fibrils, etc.) When the hybrid peptides contained a contiguous sequence of three or more lysine residues, the data could only be fit with the branched model. The average molecular weight $\langle M \rangle_w$ increased with increasing oligolysine sequence length. The average total contour length L_c of the aggregates was greater for Aβ-hybrid mixtures than for Aβ alone. The average linear density was calculated by dividing the average molecular weight by the average total contour length ($\langle M \rangle_w/L_c$); this value was ~20 kDa/nm for Aβ alone or with KLVFF-K$_1$ or KLVFF-K$_2$, but doubled to ~40 kDa/nm for Aβ with KLVFF-K$_4$ or KLVFF-K$_6$. Thus, hybrid peptides increase the molecular weight, length, extent of branching, and linear density of Aβ aggregates, with the effect becoming more pronounced as the length of the oligolysine element is increased.

$\langle M \rangle_w$ is a weighted average of contributions from monomers, oligomers, and large aggregates. The observed increase in $\langle M \rangle_w$ of Aβ aggregates in the presence of KLVFF-K$_x$ could be due to an increase in the molecular weight of the large aggregates, or to a shift in the size distribution away from monomers. To differentiate between these two possibilities, Aβ-hybrid mixtures were analyzed by size exclusion chromatography. For Aβ alone, two overlapping peaks were consistently observed, corresponding to molecular masses of the Aβ monomer (~4.3 kDa) and the Aβ dimer (~8.6 kDa). There was no measurable shift in the retention time of these two peaks with addition of hybrid peptides, suggesting that the hybrid peptides do not associate at high stoichiometric ratios with monomeric/dimeric Aβ. We calculated the fraction of putative monomers and dimers by dividing the monomer or dimer peak area by the peak area resulting from injection of Aβ without the column in place, and calculated the fraction of fibrils by difference. The size distribution was 10–15% monomer, 20–25% dimer, and ~65% fibril, and was not affected by any of the hybrid peptides (Figure 4). These results indicate that the increase in $\langle M \rangle_w$ due to the presence of hybrid inhibitors cannot be attributed to an increase in the fraction of Aβ in aggregated form; rather, the hybrid peptides increase the average size of the aggregates.

We collected and analyzed SLS data 1, 4, 24, and 48 h after mixing, or until the sample precipitated. The results,

Table 3: Size Characteristics of Aβ Aggregates in the Presence of Hybrid Peptides

	time (h)	Aβ alone	Aβ with KLVFF-K$_1$	Aβ with KLVFF-K$_2$	Aβ with KLVFF-K$_3$	Aβ with KLVFF-K$_4$	Aβ with KLVFF-K$_6$
$\langle M \rangle_w$	1	8.7	17	40	40	60	69
	4	14	28	44	49	64	—
	24	36	44	56	55	—	—
	48	46	—	—	—	—	—
L_c	1	400	960	1800	1300	1400	2000
	4	550	2000	2000	1500	1500	—
	24	1200	2300	2400	1700	—	—
	48	1600	—	—	—	—	—
l_k	1	270	140	110	130	140	130
	4	160	140	110	120	130	—
	24	140	110	110	130	—	—
	48	130	—	—	—	—	—
f	1	ND	ND	ND	4	4	5
	4	ND	3	4	4	4	—
	24	3	4	4	5	—	—
	48	4	—	—	—	—	—
$\langle M \rangle_w / L_c$	1	22	17	22	30	40	35
	4	26	14	22	30	40	—
	24	30	20	23	30	—	—
	48	30	—	—	—	—	—

FIGURE 4: Monomer (white), dimer (black), and fibril (striped) distribution of Aβ and Aβ hybrid solutions. The indicated peptide was added to Aβ peptide at 115 μM Aβ and a 1:1 Aβ:peptide molar ratio, and the mixture was injected onto a calibrated Superdex column. Peak areas were integrated to determine the relative quantity of each species. The inset shows representative chromatograms of Aβ alone (top) or with KLVFF-K$_6$ (bottom). Since the hybrid peptides cannot be detected by absorbance at 280 nm, the chromatogram shows only the elution behavior of Aβ species.

summarized in Table 3, show that, in the absence of hybrid peptides, Aβ aggregates continue to grow, eventually forming longer, thicker fibrils with a modest degree of branching. Thus, given sufficient time, the size and morphology of aggregates of Aβ alone roughly approximate those of aggregates of Aβ with effective inhibitory compounds. For example, $\langle M \rangle_w$, L_c, and f for Aβ with KLVFF-K$_6$ at 1 h and with Aβ alone at 48 h are similar. These results suggest that changes in aggregate size induced by the inhibitory peptides are primarily a matter of kinetics.

In dynamic light scattering, the diffusional properties of the particles in solution are detected, whereas in SLS, the static properties are measured. If the motion of the aggregates in solution is strictly translational diffusion of noninteracting particles, then the average hydrodynamic size of the aggregates can be calculated from the particle dimensions ($\langle M \rangle_w$, L_c, l_k, and f) using theoretical relationships (28, 29). When these calculated values were compared to the measured

values obtained by dynamic light scattering, they agreed only at early times. At later times, and especially with hybrid inhibitors possessing longer oligolysine sequences, the measured size was markedly greater than the calculated size. This is likely a reflection of attractive interaggregate interactions (or repulsive aggregate−solvent interactions) leading to formation of loose clusters of aggregates and acceleration of precipitation. Although the changes in the static properties of the aggregates caused by the inhibitory peptides appear to be primarily a matter of kinetics, as described in the previous paragraph, there are persistent differences in the dynamic (diffusional) properties. For example, although $\langle M \rangle_w$, L_c, and f are similar for Aβ with KLVFF-K$_6$ at 1 h and Aβ alone at 48 h, the hydrodynamic size is much larger for the former sample. This result suggests that attractive interactions between Aβ aggregates are stronger in the presence of the hybrid peptides.

Activity of Compounds with Variable Disrupting Element Compositions. We considered the possibility that the oligolysine-disrupting element acts by neutralizing the net charge of the Aβ aggregates. At neutral pH, Aβ has a predicted net charge of −3. Compounds with net positive charge could bind to Aβ fibrils and neutralize fibril−fibril repulsive interactions, resulting in enhanced aggregation and faster precipitation (33). Alternatively, the positively charged oligolysine sequence on the hybrid compounds could interact with negatively charged Glu-22 and Asp-23 on Aβ, near neighbors of the putative KLVFF binding site. Either of these modes of action requires that the disrupting element be positively charged. To determine whether the disrupting domain must be cationic for efficacy, we synthesized two hybrid peptides in which the lysine tetramer was replaced with glutamate (KLVFF-E$_4$, negatively charged) or serine (KLVFF-S$_4$, polar but neutral). KLVFF-E$_4$ was found to be as effective as KLVFF-K$_4$ at protecting PC-12 cells against Aβ toxicity. In contrast, KLVFF-S$_4$ was ineffective (Figure 5). For Aβ solutions containing KLVFF-E$_4$ but not KLVFF-S$_4$, the rate of aggregation was substantially increased (Figure 6A), the time required to form visible precipitates was reduced (to 26 h), and the morphology of aggregates at 1 h was altered from linear to branched (Figure 6B). Thus,
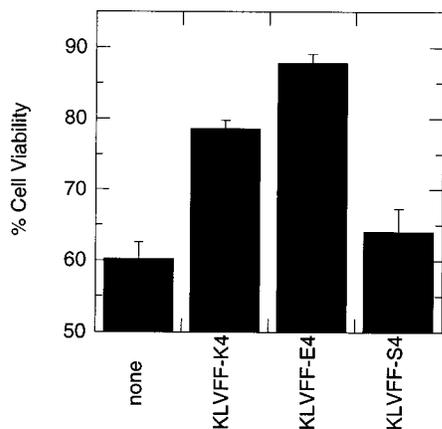
FIGURE 5: Effect of hybrid peptides with variable-charged disrupting domains on cellular toxicity of Aβ solutions. Aβ alone or with the indicated peptide was incubated for 2 days at 37 °C, and then added to plated PC-12 cells for 1 day. The Aβ concentration in wells was 25 μM, and the Aβ:hybrid molar ratio was 1:1. Cellular viability was assessed with the MTT assay. Each bar represents the mean $\pm$ standard deviation of results from two to five separate runs, with seven replicates per run.
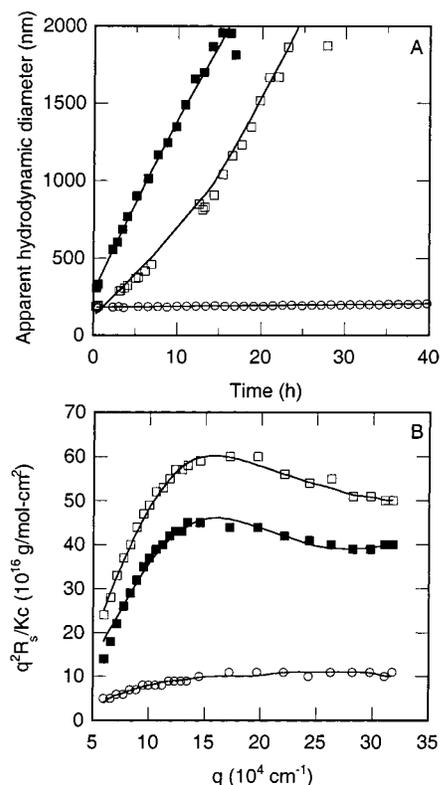
FIGURE 6: Effect of hybrid peptides with variable-charged disrupting elements on aggregation of Aβ/hybrid solutions. Aβ was mixed with the indicated peptide at 115 μM Aβ and a 1:1 Aβ:peptide molar ratio: ($\bigcirc$) Aβ with KLVFF-S$_4$, ($\square$) Aβ with KLVFF-E$_4$, and ($\blacksquare$) Aβ with KLVFF-K$_4$. (A) The average apparent hydrodynamic diameter was determined by cumulants analysis of autocorrelation functions collected at a scattering angle of 90°. (B) Kratky plots collected 1 h after mixing.

tetrameric glutamate but not serine serves as an effective disrupting element, and a positively charged disrupting element is not a requirement for hybrid peptide activity. The fact that protective activity in the toxicity assay correlated with increased aggregation kinetics suggests that KLVFF-E$_4$ acts by the same mechanism as its cationic counterparts.
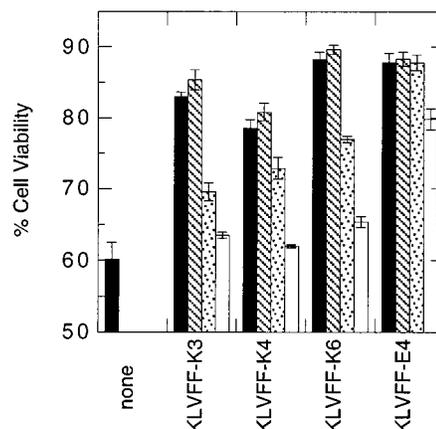
FIGURE 7: Dose dependence of cytoprotective effects of hybrid peptides. The indicated peptide was added at a 1:1 (black), 10:1 (striped), 100:1 (dotted), or 1000:1 (white) Aβ:peptide molar ratio. The Aβ concentration in wells was 25 μM. Each bar represents the mean $\pm$ standard deviation of results from two to five separate runs, with seven replicates per run.

Activity of Compounds at Low Hybrid Peptide:Aβ Ratios. We next tested whether our most potent compounds retained activity at low doses relative to Aβ concentration. A solution of Aβ with KLVFF-K$_6$ at a 1:10 hybrid:Aβ ratio was analyzed by light scattering. The rate of growth was intermediate between that with Aβ alone and that with KLVFF-K$_6$ at a 1:1 molar ratio (data not shown). The time to form visible precipitates was ~70 h, intermediate between the time required for Aβ alone versus that required for a 1:1 Aβ:KLVFF-K$_6$ ratio. On the basis of analysis of Kratky plots, the aggregates resembled those formed from solutions containing a higher concentration of KLVFF-K$_6$. Evaluation of the fitted curves yielded the following values after incubation for 1 h: $\langle M \rangle_w = (60 \pm 3) \times 10^6$ g/mol, $L_c = 1400 \pm 400$ nm, $l_k = 120 \pm 30$ nm, $f = 4 \pm 1$, and $\langle M \rangle_w/L_c = 40 \pm 10$. In comparing these results to those in Table 2, we observe that the values are not substantially different than those for Aβ with KLVFF-K$_6$ at a 1:1 molar ratio. Thus, at both equimolar and subequimolar ratios, the hybrid peptide KLVFF-K$_6$ causes similar morphological changes in Aβ fibrils, specifically, increased linear density and an increased level of branching.

To test whether peptides were capable of inhibiting Aβ toxicity at lower-than-equimolar ratios, Aβ was mixed with KLVFF-K$_3$, KLVFF-K$_4$, KLVFF-K$_6$, or KLVFF-E$_4$ at 1:1, 1:10, 1:100, and 1:1000 hybrid:Aβ molar ratios, with a constant Aβ concentration. As shown in Figure 7, protection against cellular toxicity was retained for all four hybrid peptides at a 1:10 ratio and partially or fully retained at a 1:100 ratio. KLVFF-E$_4$ was partially effective even at a 1:1000 dilution, making this one of the most potent inhibitors of Aβ toxicity reported to date.

DISCUSSION

Previously, we proposed a strategy for modular design of hybrid compounds that interfere with normal Aβ self-assembly and inhibit Aβ cellular toxicity (24). In this strategy, two components are combined: a recognition element that selectively interacts with Aβ and a disrupting element that interferes with normal self-assembly of Aβ into fibrils. To identify an effective recognition element, we

screened several peptides that were partially homologous to Aβ and found that an element comprising residues 16−20 of Aβ, KLVFF, when coupled to a hexameric lysine-disrupting element, functioned as an effective inhibitor of Aβ toxicity (*10*). Here we use KLVFF as the recognition element to explore the structural requirements of the disrupting element. Our goal is to define the structural features required for inhibitory activity, and to further understand the mode of action of this new class of inhibitors. Peptides that block the cellular toxicity of Aβ serve as potential lead compounds for development of therapeutics, and as probes for investigating the molecular basis for the link between Aβ aggregation and Aβ toxicity.

Starting with the compound KLVFF-K$_6$, we synthesized a series of peptides in which the oligolysine-disrupting element was shortened systematically. Peptides with three to six lysines in the disrupting element were equally effective at inhibiting Aβ toxicity, when evaluated on the basis of inhibition of MTT toxicity at a 1:1 Aβ:peptide molar ratio. The level of protection decreased for compounds possessing only one or two lysines in the disrupting sequence. Compounds with a disrupting domain of three or more lysine residues retained full inhibitory activity at a 1:10 Aβ:peptide molar ratio; at a 1:100 ratio, KLVFF-K$_6$ was slightly more effective than KLVFF-K$_3$ or KLVFF-K$_4$. These data indicate that three or four lysine contiguous residues are sufficient disrupting elements.

Compounds with oligolysine-disrupting elements were further evaluated for their effect on Aβ aggregation. All compounds increased the rate of aggregation and decreased the time to precipitation, with the effect being proportional to the number of lysines in the disrupting element of the hybrid peptide. There was a striking correlation between increased aggregation kinetics and an increased level of protection against toxicity. Protective compounds appear to both facilitate the growth of Aβ aggregates and enhance interaggregate association.

We next investigated whether there were specific compositional features required for an effective disrupting element. Compounds with an anionic disrupting element, KLVFF-E$_4$, and a polar neutral disrupting element, KLVFF-S$_4$, were synthesized and tested. KLVFF-E$_4$ was as effective as its cationic counterpart at inhibiting Aβ toxicity. Intriguingly, this hybrid peptide also increased growth rates and changed aggregate morphology. In sharp contrast, KLVFF-S$_4$ was completely ineffective, affecting neither Aβ aggregation nor Aβ toxicity. These results rule out the possibility that specific Coulombic interactions requiring a cationic element are needed for disruption. Besides the absence of charge, the serine side chain differs from that of glutamate and lysine in several ways; it is smaller and less hydrophilic and carries fewer waters of hydration (*34, 35*). It is possible that KLVFF-K$_4$ and KLVFF-E$_4$ bind equally well to Aβ and that KLVFF-S$_4$ binds only weakly or not at all. Alternatively, the three compounds may bind to Aβ equally well. One can readily imagine that the growing fibril can accommodate the small, neutral serine side chains with little disruption, whereas the larger, charged, hydrated lysine and glutamate side chains are not easily buried. This model would indicate that effective disruption is achieved by interfering with the regular templated growth of Aβ fibrils.

Aβ molecules may interact with each other through binding at the KLVFF region (*36, 37*). Our hybrid peptides might bind by aligning their recognition element (KLVFF) with the KLVFF sequence of Aβ. With an effective disrupting element, another Aβ molecule might partially assemble on the KLVFF template, but would not be able to make tight contact with adjacent hydrophobic domains on Aβ. This would leave a hydrophobic surface exposed, like a kink in an otherwise linear chain, thus facilitating branching and fibril−fibril association.

Our inhibitory compounds act not by limiting the formation of Aβ aggregates but rather by increasing the rates of aggregation and precipitation. Significant evidence has accumulated that indicates Aβ is toxic only in its aggregated form. An emerging view is that the toxic species is an intermediate in the pathway that leads to insoluble fibrils, rather than the insoluble fibrils themselves (*10−12*). Our data directly support this hypothesis. This finding is significant because it leads to the conclusion that compounds need not block the initial aggregation step to be effective. Thus, agents that can interact with and disarm the soluble aggregates may serve as useful therapeutic leads.

The ability of our inhibitory compounds to facilitate Aβ aggregation suggests that they interact with multiple copies of Aβ. This mode of interaction is promising, because it does not demand that one or more copies of the inhibitor bind to Aβ, which is the stoichiometry presumably required to completely prevent aggregation. Indeed, our effective compounds retained full protective activity with a 10-fold excess of Aβ (10:1 Aβ: inhibitor ratio) and partial to full activity even at a 100-fold excess of Aβ. This result highlights the advantages of these agents over others that required equimolar or greater ratios for full protection against Aβ toxicity (*19−21*). With their unique mechanism of action, these hybrid peptides function as some of the most effective inhibitors of Aβ toxicity reported to date.

REFERENCES

1. Kirschner, D. A., Abraham, C., and Selkoe, D. J. (1986) *Proc. Natl. Acad. Sci. U.S.A. 83*, 503−507.
2. Polvikoski, T., Sulkava, R., Haltia, M., Kainulained, K., Vuorio, A., Verkkoniemi, A., Niinisto, L., Halonenm, P., and Kontula, K. (1995) *N. Engl. J. Med. 333*, 1242−1247.
3. Selkoe, D. J. (1997) *Science 275*, 630−631.
4. Rubinsztein, D. C. (1997) *Prog. Neurobiol. 52*, 447−454.
5. Holcomb, L., Gordon, M. N., McGowan, E., Yu, X., Benkovic, S., Jantzen, P., Wright, K., Saad, I., Mueller, R., Morgan, D., Sanders, S., Zehr, C., O'Campo, K., Hardy, J., Prada, C.-M., Eckman, C., Younkin, S., Hsiao, K., and Duff, K. (1998) *Nat. Med. 4*, 97−100.
6. Hsiao, K., Chapman, P., Nilsen, S., Eckman, C., Harigaya, Y., Younkin, S., Yang, F., and Cole, G. (1996) *Science 274*, 99−102.
7. Pike, C. J., Burdick, D., Walencewicz, A. J., Glabe, C. G., and Cotman, C. W. (1993) *J. Neurosci. 13*, 1676−1687.
8. Simmons, L. K., May, P. C., Tomaselli, K. J., Rydel, R. E., Fuson, K. S., Brigham, E. F., Wright, S., Lieberburg, I., Becker, G. W., Brems, D. N., and Li, W. (1994) *Mol. Pharmacol. 45*, 373−379.

9. Seilheimer, B., Bohrmann, B., Bondolfi, L., Muller, F., Stuber, D., and Dobeli, H. (1997) *J. Struct. Biol. 119*, 59−71.

10. Pallitto, M. M., Ghanta, J., Heinzelman, P., Kiessling, L. L., and Murphy, R. M. (1999) *Biochemistry 38*, 3570−3578.

11. Lansbury, P. T., Jr. (1999) *Proc. Natl. Acad. Sci. U.S.A. 96*, 3342−3344.

12. Koo, E. H., Lansbury, P. T., Jr., and Kelley, J. W. (1999) *Proc. Natl. Acad. Sci. U.S.A. 96*, 9989−9990.

13. Roher, A. E., Chaney, M. O., Kuo, Y.-M., Webster, S. D., Stine, W. B., Haverkamp, L. J., Woods, A. S., Cotter, R. J., Tuohy, J. M., Krafft, G. A., Bonnell, B. S., and Emmerling, M. R. (1996) *J. Biol. Chem. 271*, 20631−20635.

14. Lambert, M. P., Barlow, A. K., Chromy, B. A., Edwards, C., Freed, R., Liosatos, M., Morgan, T. E., Rozovky, I., Trommer, B., Viola, K. L., Wals, P., Zhang, C., Finch, C. E., Krafft, G. A., and Klein, W. L. (1998) *Proc. Natl. Acad. Sci. U.S.A. 95*, 6448−6453.

15. Hartley, D. M., Walsh, D. M., Ye, C. P., Diehl, T., Vasquez, S., Vassilev, P. M., Teplow, D. B., and Selkoe, D. S. (1999) *J. Neurosci. 19*, 8876−8884.

16. Ward, R. V., Jennings, K. H., Jepras, R., Neville, W., Owen, D. E., Hawkins, J., Christie, G., Davis, J. B., George, A., Karran, E. H., and Howlett, D. R. (2000) *Biochem. J. 348*, 127−144.

17. Lorenzo, A., and Yankner, B. A. (1994) *Proc. Natl. Acad. Sci. U.S.A. 91*, 12243−12247.

18. Kisilevsky, R., Lemieux, L. J., Fraser, P. E., Kong, X., Hultin, P. G., and Szarek, W. A. (1995) *Nat. Med. 1*, 143−148.

19. Klunk, W. E., Debnath, M. L., Koros, A. M. C., and Pettegrew, J. W. (1998) *Life Sci. 63*, 1807−1814.

20. Howlett, D. R., George, A. R., Owen, D. E., Ward, R. V., and Markwell, R. E. (1999) *Biochem. J. 343*, 419−423.

21. Tomiyama, T., Shoji, A., Kataoka, K.-I., Suwa, Y., Asano, S., Kanetko, H., and Endo, N. (1996) *J. Biol. Chem. 271*, 10205−10208.

22. Howlett, D. R., Perry, A. E., Godfrey, F., Swatton, J. E., Jennings, K. H., Spitzfaden, C., Wadsworth, B., Wood, S. J., and Markwell, R. E. (1999) *Biochem. J. 340,* 283−289.

23. Kuner, P., Bohrmann, B., Tjernberg, L. O., Naslund, J., Huber, G., Celenk, S., Gruninger-Leitch, F., Richards, J. G., Jakob-Roetne, R., Kemp, J. A., and Nordstedt, C. (2000*) J. Biol. Chem. 275*, 1673−1678.

24. Ghanta, J., Shen, C.-L., Kiessling, L. L., and Murphy, R. M. (1996) *J. Biol. Chem. 271*, 29525−29528.

25. Soto, C., Kindy, M. S., Baumann, M., and Frangione, B. (1996) *Biochem. Biophys. Res. Commun. 226*, 672−680.

26. Tjernberg, L. O., Näslund, J., Lindqvist, F., Johansson, J., Karlström, A. R., Thyberg, J., Terenius, L., and Nordstedt, C. (1996) *J. Biol. Chem. 271*, 8545−8548.

27. Findeis, M. A., Musso, G. M., Arico-Muendel, C. C., Benjamin, H. W., Hundal, A. M., Lee, J.-J., Chin, J., Kelley, M., Wakefield, J., Hayward, N. J., and Molineaux, S. M. (1999) *Biochemistry 38*, 6791−6800.

28. Shen, C.-L., Fitzgerald, M. C., and Murphy, R. M. (1994) *Biophys. J. 65*, 2383−2395.

29. Shen, C.-L., and Murphy, R. M. (1995) *Biophys. J. 69*, 640−651.

30. Koyama, R. (1973) *J. Phys. Soc. Jpn. 34*, 1029−1038.

31. Huber, K., and Burchard, W. (1989) *Macromolecules 22*, 3332−3336.

32. Burchard, W. (1983) *Adv. Polym. Sci. 48*, 1−124.

33. Tang, J. X., Ito, T., Tao, T., Trabu, P., and Janmey, P. A. (1997) *Biochemistry 36*, 12600−12607.

34. Darby, N. J., and Creighton, T. E. (1993) *Protein Structure*, Oxford University Press, Oxford, U.K.

35. Kuntz, I. D., Jr., and Kauzmann, W. (1974) *Adv. Protein Chem. 28*, 239.

36. Tjernberg, L. O., Lilliehook, C., Callaway, D. J. E., Naslund, J., Hahne, S., Thyberg, J., Terenius, L., and Nordstedt, C. (1997) *J. Biol. Chem. 272*, 12601−12605.

37. Benzinger, T. L. S., Gergory, D. M., Burkoth, T. S., Miller-Auer, H., Lynn, D. G., Botto, R. E., and Meredith, S. C. (2000) *Biochemistry 39*, 3491−4399.